



## Occurrence characteristics of mesospheric gravity waves at 51°N

D. H. Giers,<sup>1\*</sup> Y. Sahai,<sup>1†</sup> L. L. Cogger<sup>1</sup> and E. H. Ryan<sup>2</sup>

<sup>1</sup>Canadian Network for Space Research, Department of Physics and Astronomy, University of Calgary, Calgary, Alberta, T2N 1N4, Canada; <sup>2</sup>Department of Meteorology and Physical Oceanography, Rosenstiel School of Marine and Atmospheric Science, The University of Miami, 4600 Rickenbacker Causeway, Miami, FL 33149, U.S.A.

(Received in final form 27 August 1996; accepted 29 August 1996)

**Abstract**—Observations of the OH(8-3) band rotational temperature have been carried out from Calgary (51°N, 114°W), Canada, from 1988 to 1990. The measurements have been taken in orthogonal scanning mode and the data set has been analyzed to study salient features of gravity waves in the mesospheric region from this mid-latitude station. Rotational temperature data from 36 nights showed distinct gravity wave activity during this period. The gravity wave characteristics studied include the dominant period, horizontal structure speed, implied horizontal wavelength and horizontal component of direction of propagation. The preferred direction in the horizontal wave propagation at Calgary is towards the north-west. A comparison of the observed horizontal propagation directions with the permitted directions, using model wind profiles for Calgary, shows good agreement. This indicates that the upward flow of wave energy could be modified by the background wind. © 1997 Elsevier Science Ltd

### INTRODUCTION

Viereck (1991) has recently reviewed the mesospheric dynamics and chemistry. Gravity waves play an important role in determining the dynamics and structure of the mesospheric region. During recent years there has been considerable interest in investigations related to gravity waves in the mesospheric region using nightglow (Hecht *et al.*, 1987; Taylor *et al.*, 1987, 1991, 1993; Cogger *et al.*, 1988; Viereck and Deehr, 1989; Swenson *et al.*, 1990; Wiens *et al.*, 1993; Kieffaber *et al.*, 1993), radar (Reid, 1986; Reid and Vincent, 1987; Manson and Meek, 1988; Manson, 1990) and lidar (Gardner and Voelz, 1987; Senft and Gardner, 1991; Beatty *et al.*, 1992) observations. In this article, we present and discuss the occurrence characteristics of gravity waves in the mesospheric region observed at Calgary (51°N, 114°W), Canada, using the rotational temperatures determined from the scanning (north-south and west-east) observations of the OH (8-3) band nightglow emission. The data presented span the period from 1988 to 1990. Some

features of the mesospheric gravity waves studies based on the earlier observations at Calgary have been presented by Cogger *et al.* (1988) and Elphinstone *et al.* (1988).

### INSTRUMENTATION

The north-south (N-S) and west-east (W-E) scanning observations of the OH (8-3) band emission were made with a multichannel tilting filter photometer (Meriwether, 1975; Meriwether *et al.*, 1983). The photometer has a full angle field of view of 3° and each interference filter has a diameter of 2 inches. The photomultiplier is a cooled (-20°C) red sensitive EMI 9658B and is operated in pulse detection mode.

A positionable double-axis azimuth-zenith mirror system has been used for orthogonal scanning observations. The system was programmed to observe at 15 discrete sky positions, in each north-south and west-east scan directions. The maximum off-zenith angle of observations used was 27° and the separations between the discrete observation positions were chosen to give a spatial resolution of 6 km at an altitude of 85 km. The maximum off zenith angle of 27° allows a total scanning range of about 90 km on the OH layer. Thus we are unable to measure the size of waves much larger than this. The photometer operation and data acquisition were carried out by a PDP 11/23 minicomputer.

\*Present address: Gemini Optics Consulting Services, 72 MacEwan Park Road N.W., Calgary, Alberta, T2K 3E9, Canada.

†Present address: Instituto Nacional de Pesquisas Espaciais (INPE), 12201-970, São José Dos Campos, SP, Brazil. Corresponding author.

The photometer provides near simultaneous scanning observations of the OI 630.0 and 557.7 nm and OH(8-3) band nightglow emissions. In order to determine the rotational temperature of the OH (8-3) band (hereafter T(OH)), measurements were made of the  $P_1(2)$  and  $P_1(5)$  rotational lines at wavelengths 731.6 and 740.1 nm, respectively. Each of these line measurements was accompanied by a continuum background measurement obtained by tilting the filter. Narrow band (0.3 nm) interference filters have been used for these measurements. Details related to the determination of the OH rotational temperature have been described by Meriwether (1975). Estimated errors in T(OH) are approximately  $\pm 5$  K. One complete scan cycle of the observations for the three emissions takes about 20 min.

#### DATA ANALYSIS: GRAVITY WAVE CHARACTERISTICS

To study the occurrence characteristics of gravity waves, the data obtained from the orthogonal scanning observations for each night were divided into two sets, one set being the spatial variation of the rotational temperature and the other being the temporal variation of the rotational temperature. Both of these data sets have components in the north-south and west-east directions. These data sets were studied in detail to determine which nights showed the presence of distinct gravity wave activity. Several examples of the rotational temperature data showing gravity wave activity and simultaneous measurements of the OI 557.7 nm emission during the presence of OH temperature waves from this location have been presented by Cogger *et al.* (1988; Figs 1, 2 and 3). Nights when the data may have been contaminated by auroral activity or bad weather were discarded.

The next step in the processing was to calculate the velocity spectra using the technique described by Elphinstone *et al.* (1986, 1988), in both the north-south and west-east directions, in order to determine the meridional and zonal velocities, respectively, of the moving mesospheric thermal structure.

Velocity spectral analysis can be carried out in several ways and many investigators have done this in the past. Briggs (1984) reviewed how a full correlation analysis technique could be used for determining the motion of a two-dimensional pattern. However, restrictions apply when utilizing such a technique, when more than three spatial points are used to collect the data, as in the present case. These additional locations imply an over-specification of the physical features. To include all the information requires the application of a linear least squares fitting technique.

Other techniques for the determination of velocity information have also been utilized, such as that by Clairemidi *et al.* (1985), who were able to define velocities as well as wavelengths from a comparative study of photographic plates of the upper atmospheric infrared OH airglow structure. However, such measurements are now readily obtained by imagers (e.g. Taylor *et al.*, 1993), which are now the primary source of this type of information. Freund and Jacka (1979) approached the analysis of two-dimensional upper atmospheric moving forms in a manner which is similar to that used in this study. They determined the best velocity between time series with various spatial separations and found the best fit velocity from these.

The procedure utilized here was to search the data set for a wide range of possible velocities which are defined by the sampling and find the velocity which best fits all of the combinations of time series which are a part of the input data set. For each night there are two velocities which are found; these are the meridional velocity,  $V_{meridional}$ , and the zonal velocity,  $V_{zonal}$ . The data analysis assumes that the wave motions are monochromatic and that there was only one main wave disturbance for each night.

The velocities which are deduced in the analysis are not necessarily the true phase speeds of the waves, but are the speeds at which the upper atmospheric thermal patterns are moving in the horizontal direction. Figure 1 shows a schematic of a horizontally moving wave pattern, moving with a velocity of  $V_{structure}$  ( $V_{st}$ ). This figure illustrates how the meridional and zonal velocities are related to the structure velocity. If the pattern moves from the origin to a point  $y_1$  in the meridional direction in a time  $t_1$  then:

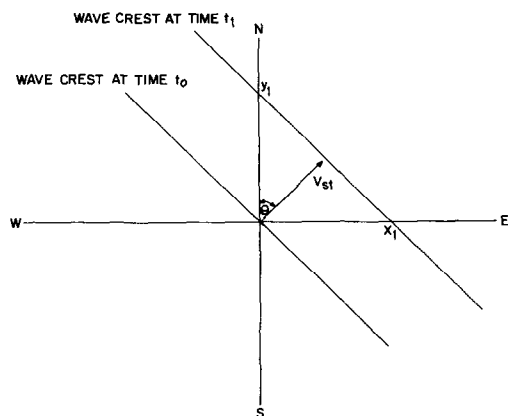


Fig. 1. Schematic representation of a horizontally moving pattern for the determination of structure velocity.

$$t_1 = \frac{y_1 \cos \theta}{V_{st}} \quad (1)$$

and similarly in the zonal direction the time taken for the pattern to move from the origin to a point  $x_1$  is given as:

$$t_1 = \frac{x_1 \sin \theta}{V_{st}} \quad (2)$$

where  $V_{st}$  is the speed of the moving structure.

Hence, the velocity components which are observed and which are deduced in the analysis are actually:

$$V_{meridional} = \frac{y_1}{t_1} \quad (3)$$

and

$$V_{zonal} = \frac{x_1}{t_1} \quad (4)$$

These components are related to the speed of the moving upper atmospheric thermal structure as:

$$V_{meridional} = \frac{V_{st}}{\cos \theta} \quad (5)$$

$$V_{zonal} = \frac{V_{st}}{\sin \theta} \quad (6)$$

where the angle of the horizontal direction of propagation,  $\theta$ , is measured in a clockwise fashion from cardinal north. This angle of propagation of the moving upper atmospheric thermal structure is determined by:

$$\tan \theta = \frac{V_{meridional}}{V_{zonal}} = \frac{y_1}{x_1} \quad (7)$$

and the magnitude of the structure velocity  $V_{st}$  is given by:

$$V_{st} = \frac{V_{zonal} V_{meridional}}{\sqrt{V_{zonal}^2 + V_{meridional}^2}} = \frac{y_1}{t_1} \cos \theta \quad (8)$$

Therefore, from the measurement of both the meridional and zonal velocities, the magnitude and direction of the structure velocity of the moving gravity wave pattern can be determined.

Further processing to yield frequency information was done by implementing a one-dimensional maximum entropy spectral analysis technique (see Cogger *et al.* (1988) for details of the technique). The algorithm for this specific type of analysis has been presented by Ulrych and Bishop (1975). A spectral analysis of this type yields the power spectrum as a function of frequency between zero and the Nyquist limit. Prior to this analysis being carried out, a first order difference filter is implemented, so that the d.c. component present in the data is removed.

This analysis provides estimates of the frequency of the periodic fluctuations being studied. For each night of useful photometer data a power spectrum was calculated for each temporal scan (yielding frequency information). These were all normalized such that the integrated value of the spectrum was equal to one. For any single night the respective power spectra were averaged together to give a single power spectrum in time for the entire night's data set. Error bars on the power spectra were found by finding the standard deviation of the mean at any given point.

The velocity spectral analysis and the maximum entropy spectral analysis carried out in this study determined the principal meridional and zonal velocities, and the principal period, respectively, for each night of data. The analysis of the photometer-acquired data could only yield observed periods,  $T_{obs}$  of upper atmospheric fluctuations with values of between 30 and 450 min because of the sampling of the data and the temporal length of the scan.

The implied horizontal wavelength,  $\lambda_h$ , was calculated using the product of the observed period,  $T_{obs}$ , and the observed structure velocity,  $V_{st}$ , as:

$$\lambda_h = T_{obs} V_{st} \quad (9)$$

## RESULTS AND DISCUSSION

Distinct monochromatic gravity waves were observed on 36 nights during the period 1988–90. Results from these nights are reported in this paper. It should be mentioned that, because of instrumental problems, very few nights of observations were obtained during 1989. The data set has vastly more observations during the winter months than the rest of the year because of cloud cover as a function of local season. As pointed out earlier by Cogger *et al.* (1988), about one-third of the uncontaminated nights show wave activity. The gravity wave characteristics presented include the observed period ( $T_{obs}$ ), the horizontal phase velocity ( $V_{st}$ ), the implied horizontal wavelength ( $\lambda_h$ ), and the horizontal component of the direction of propagation.

In Figs 2, 3 and 4 and 6 we have plotted histograms of the frequency of occurrence of the observed periods, the horizontal structure speeds, the implied horizontal wavelengths, and directions of propagation, respectively. Figure 2 shows that the observed periods are between 30 and 190 min and fall in the range of those reported from other mid- and high-mid-latitude locations (Gardner and Voelz, 1987; Manson and Meek, 1988). The observed periods show a maximum between 50 and 90 min.

Figure 3 shows that the observed horizontal struc-

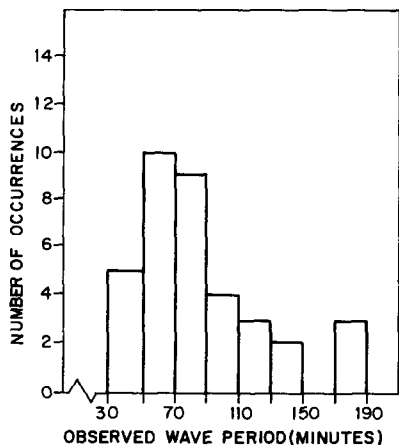


Fig. 2. Histogram of the observed gravity wave periods (1988–1990).

ture speeds lie in the range  $10\text{--}70\text{ m s}^{-1}$ , peaking at  $20\text{--}30\text{ m s}^{-1}$ . The observed range of speeds is comparable to those reported by Manson and Meek (1988); however, they have included background wind data in their analysis and reported a rather flat distribution.

The occurrence characteristics of the implied horizontal wavelengths are plotted in Fig. 4. For  $\lambda_h$ , the range lies between 40 and 320 km. This is consistent with lidar and radar measurements (Gardner and Voelz, 1987; Manson and Meek, 1988).

The polar plots of the observed horizontal structure velocities are shown in Fig. 5. The occurrence frequency of the observed horizontal velocities in different segments are shown in Fig. 6. A perusal of Figs 5 and 6 indicates that the preferred direction of hori-

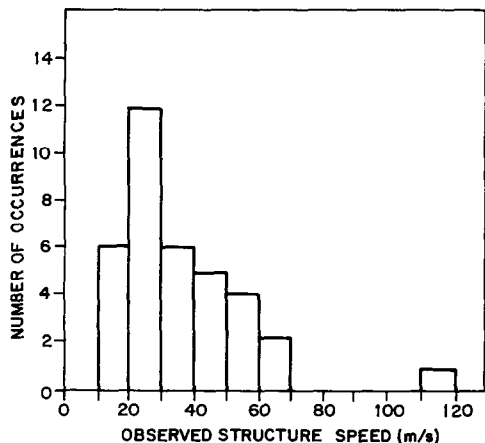


Fig. 3. Histogram of the observed gravity wave horizontal structure speeds (1988–1990).

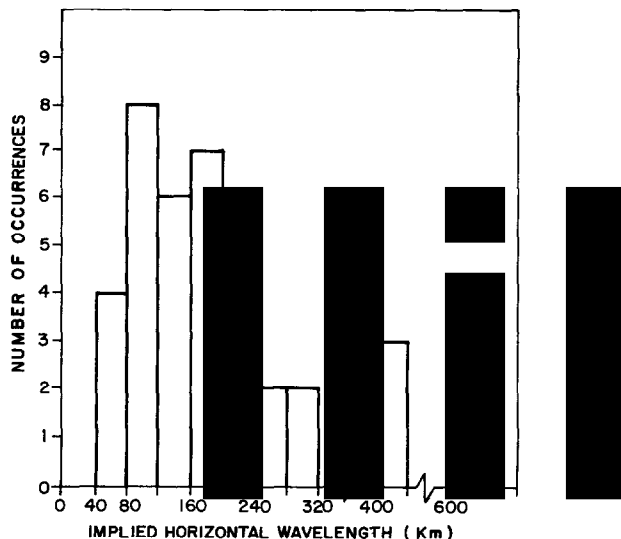


Fig. 4. Histogram of the implied horizontal wavelengths (1988–1990).

zonal wave propagation is towards the north–west. A similar tendency for northward propagation using OH emission imaging observations has also been reported by Taylor *et al.* (1993) from measurements carried out in Colorado ( $40^\circ\text{N}$ ,  $106^\circ\text{W}$ ), U.S.A. However, the radar observations reported by Manson and Meek (1988) from Saskatoon show the strongest variation to be in the southward direction. It is rather surprising that two different observation techniques show opposite characteristics in the propagation direction at locations not far from each other. This needs further investigation, possibly with simultaneous measurements using different observational techniques.

Using the wind profiles (Ryan, 1991; Ryan and Tuan, 1991) model for Calgary, background wind blocking diagrams (Taylor *et al.*, 1993) were plotted for the months of January and February (we selected months during which there have been most nights of observations). Figure 7 shows the blocking diagram for local midnight conditions during the months of January and February (winter) at 85 km. The shaded area represents the forbidden region of wave propagation caused by horizontal winds in the lower atmosphere. Also shown are the horizontal propagation directions and magnitudes of the observed gravity waves. As mentioned earlier, we have not considered nights with auroral contamination and, therefore, gravity waves of auroral origin (Chandra *et al.*, 1979) are unlikely to have been the cause of the observed wave activity in the present study. It is observed from

Velocity Vector Plot For 1988 1989 1990

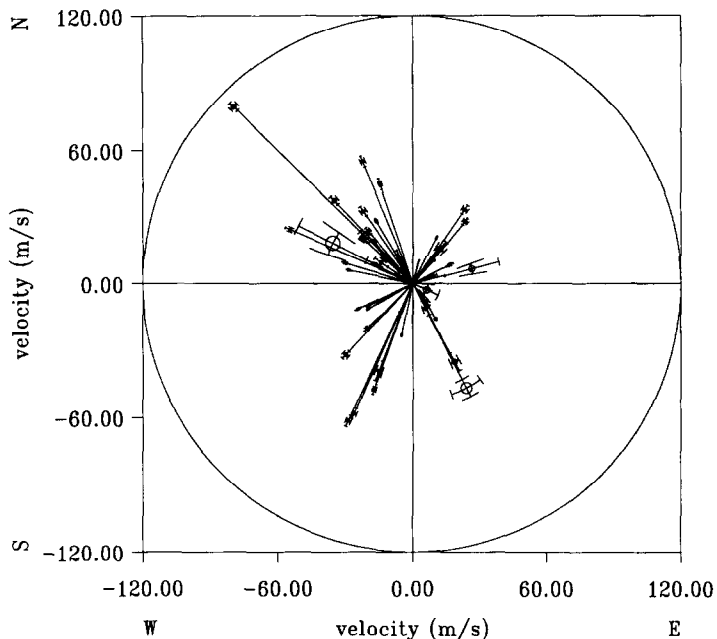


Fig. 5. Velocity vector plot of the horizontal component of the direction of propagation (1988-1990).

Fig. 7 that there is a good agreement between the observed directions of wave propagation and permitted regions in the blocking diagram. These results are both consistent with and supplement those reported by Taylor *et al.* (1993), who have discussed in detail the influence of the middle atmospheric winds on the azimuthal distribution of gravity waves reach-

ing the upper atmosphere from an origin in the troposphere. The data of Taylor *et al.* (1993) indicated shorter periods than most of those presented here (probably caused by the temporal resolution) and thus

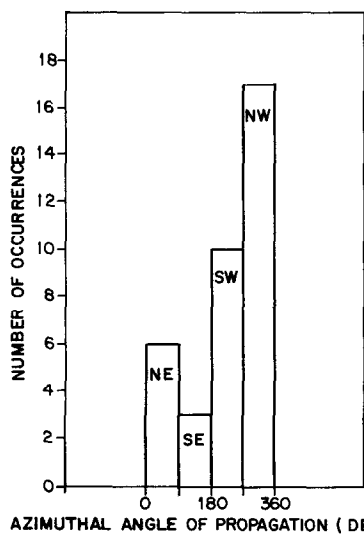


Fig. 6. Histogram showing the quadrant of horizontal propagation of the observed gravity waves (1988-1990).

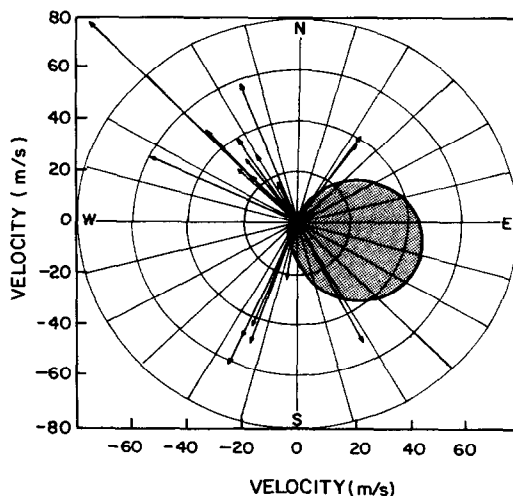


Fig. 7. Blocking diagram at 85 km at local midnight for January and February (winter conditions). The restricted region for gravity wave propagation to the OH emission layer height is indicated as the shaded region. The arrows show the magnitudes and directions of the gravity wave motions observed.

are quite complementary. Where the results reported by Taylor *et al.* (1993) were for May, June and July (summer) with most of the blocking occurring to the west and the observed waves propagating to the east, these results are for January and February (winter) where the winds are predominantly to the east and the observed waves are propagating to the west. This reinforces the conclusion that wind filtering is blocking the upward flow of wave energy.

### CONCLUSIONS

Using the rotational temperatures determined from scanning observations of the OH(8-3) band nightglow emission, we have presented the occurrence characteristics of several gravity wave parameters at 51°N. The principal features are summarized below.

1. The observed periods are in the range of 30–190 min and show a maximum between 50 and 90 min.

2. The observed horizontal structure speeds lie in the range of 10–70 m s<sup>-1</sup>, peaking at 20–30 m s<sup>-1</sup>.
3. The implied horizontal wavelengths are in the range of 40–320 km.
4. The preferred direction for the horizontal wave propagation at Calgary is towards the north-west.
5. Superpositions of the observed horizontal propagation directions and magnitudes for the months of January and February on a 'blocking diagram', using model wind profiles for Calgary, show good agreement, which indicates that the upward flow of wave energy could be modified by the background winds.

*Acknowledgements*—One of the authors (Y.S.) would like to thank Professor L. L. Cogger for kindly arranging the financial support for his visit to the University of Calgary. The work was supported by CNPq, Brazil, grant 202248/91(NV), by the Canadian Network for Space Research, and by a grant from the Natural Sciences and Engineering Research Council of Canada.

### REFERENCES

- |  |      |   |
|--|------|---|
| Beatty T. J., Hostetler C. A. and Gardner C. S.  | 1992 | Lidar observations of gravity wave, and their spectra near the mesopause and stratopause at Arecibo. <i>J. Atmos. Sci.</i> <b>49</b> , 477–496.                                   |
| Briggs B. H.   | 1984 | The analysis of spaced sensor records by correlation techniques, <i>Handbook for MAP</i> , (Vincent R. A., ed.) SCOSTEP Secretariat, University of Illinois, Urbana, pp. 168–186. |
| Chandra S., Krankowsky K., Lammerz P. and Spencer N. W.                                  | 1979 | Auroral origin of medium scale gravity waves in neutral composition and temperature. <i>J. geophys. Res.</i> <b>84</b> , 1891–1897.   |
| Clairemidi J., Herse M. and Morcels G.   | 1985 | Bi-dimensional observation of waves near the mesopause at auroral latitudes. <i>Planet. Space Sci.</i> <b>33</b> , 1013–1022.   |
| Cogger L. L., Elphinstone R. D. and Giers D. H.  | 1988 | Wave characteristics obtained from OH rotational temperatures and 557.7 nm airglow intensities. <i>J. atmos. terr. Phys.</i> <b>50</b> , 943–950.                                 |
| Elphinstone R. D., Murphree J. S. and Cogger L. L.                                       | 1986 | A technique for the analysis of two-dimensional data: application to OI 5577 Å airglow. <i>J. atmos. terr. Phys.</i> <b>48</b> , 213–220.   |
| Elphinstone R. D., Cogger L. L., Murphree J. S., Murty G. S. N. and Meriwether J. W. Jr. | 1988 | The analysis of hydroxyl rotational temperatures to characterize moving thermal structures near the mesopause. <i>J. Atmos. terr. Phys.</i> <b>50</b> , 657–688.                  |
| Fruend J. T. and Jacka F.  | 1979 | Structure in the 557.7 nm OI airglow. <i>J. atmos. terr. Phys.</i> <b>41</b> , 25–31.   |
| Gardner C. S. and Voelz D. C.  | 1987 | Lidar studies of the nighttime sodium layer over Illinois. 2: gravity waves. <i>J. geophys. Res.</i> , <b>92</b> , 4673–4594.   |
| Hecht J. H., Walterscheid R. L., Sivjee G. G., Christensen A. B. and Pranke J. B.        | 1987 | Observations of wave-driven fluctuations of OH nightglow emission from Sondre Stromfjord, Greenland. <i>J. geophys. Res.</i> <b>92</b> , 6091–6099.                               |
| Kieffaber L. M., Friesen D. R., Knutson L. and Peterson A. W.                            | 1993 | Short gravity wave periodicities during AIDA. <i>J. atmos. terr. Phys.</i> <b>55</b> , 341–354.   |
| Manson A. H.   | 1990 | Gravity wave horizontal and vertical wavelengths: an update of measurements in the mesopause region (80–100 km). <i>J. Atmos. Sci.</i> <b>47</b> , 2765–2773.                     |

- Manson A. H. and Meek C. E. 1988 Gravity wave propagation characteristics (60–120 km) as determined by the Saskatoon MF radar (GRAVNET) system: 1983–85 at 52°N, 107°W. *J. Atmos. Sci.* **45**, 932–946.
- Meriwether J. W. Jr. 1975 High latitude airglow observations of correlated short-term fluctuations in the hydroxyl Meinel 8-3 band intensity and rotational temperature. *Planet. Space Sci.* **23**, 1211–1221.
- Meriwether J. W. Jr., Tepley C. A., Prince S. A., Hays P. B. and Cogger L. L. 1983 Remote ground-based observations of terrestrial airglow emissions and thermospheric dynamics at Calgary, Alberta, Canada. *Opt. Eng.* **22**, 128–131.
- Reid I. M. 1986 Gravity wave motions in the upper middle atmosphere (60–110 km). *J. atmos. terr. Phys.* **48**, 1057–1072.
- Reid I. M. and Vincent R. A. 1987 Measurements of mesospheric gravity wave momentum fluxes and mean flow accelerations at Adelaide, Australia. *J. atmos. terr. Phys.* **49**, 443–460.
- Senft D. C. and Gardner C. S. 1991 Seasonal variability of gravity wave activity and spectra in the mesopause region at Urbana. *J. geophys. Res.* **96**, 17229–17264.
- Swenson G. R., Mende S. B. and Geller S. P. 1990 Fabry–Perot imaging of OH(8-3): rotational temperatures and gravity waves. *J. geophys. Res.* **95**, 12251–12264.
- Taylor M. J., Hapgood M. A. and Rothwell P. 1987 Observation of gravity wave propagating in the OI (557.7 nm), Na (589.2 nm) and the near infrared OH nightglow emissions. *Planet. Space Sci.* **35**, 413–428.
- Taylor M. J., Espy P. J., Baker D. J., Sica R. J., Neal P. C. and Pendleton W. R. Jr. 1991 Simultaneous intensity, temperature and imaging measurements of short period wave structure in the OH nightglow emission. *Planet. Space Sci.* **39**, 1171–1188.
- Taylor M. J., Ryan E. H., Tuan T. F. and Edwards R. 1993 Evidence of preferential directions for gravity wave propagation due to wind filtering in the middle atmosphere. *J. geophys. Res.* **98**, 6047–6057.
- Ulrych T. J. and Bishop T. N. 1975 Maximum entropy spectral analysis and autoregressive decomposition. *Rev. Geophys. Space Phys.* **13**, 183–200.
- Viereck R. A. 1991 A review of mesospheric dynamics and chemistry. *Rev. Geophys. Supplement U.S. National Report* **29**, 1132–1142.
- Viereck R. A. and Deehr C. S. 1989 On the interaction between gravity waves and the OH Meinel (6-2) and the O<sub>2</sub> atmospheric (0-1) bands in the polar night airglow. *J. geophys. Res.* **94**, 5397–5404.
- Wiens R. H., Zhang S. P., Peterson R. N., Shepherd G. G., Tepley C. A., Kieffaber L., Niciejewski R. and Hecht J. H. 1993 Simultaneous optical observations of long-period gravity waves during AIDA 89. *J. atmos. terr. Phys.* **55**, 325–430.
- Reference is also made to the following unpublished material*
- Ryan E. H. 1991 Critical layer directional filtering of atmospheric gravity waves: A comparison of airglow observation and a wind profile model, M.S. Thesis. The University of Cincinnati, Ohio.
- Ryan E. H. and Tuan T. F. 1991 Gravity waves blocking by critical layers, paper presented at Middle Atmosphere Periodic Structure and Associated Radiance (MAPSTAR) Meeting, Air Force Geophysics Laboratory, Boston, Mass., April 22–23, 1991.